The Egyptian Journal of Hospital Medicine (October 2017) Vol.69(1), Page 1680-1691

Role of Diffusion Weighted MRI Sequence in Evaluation of Cholangiocarcinoma

Ahmed H. E. Ismail[1], Yasser A. M. Abd El Mawla[2], Amr M. Abd El Samad[2,] Mohamed F. Hussein[1]
[1]Theodor Bilharz Research Institute, [2]Faculty of Medicine, Ain Shams University
Corresponding author: Ahmed Hamdy El Sayed dr.ahmed.hamdy.elsayed@gmail.com

ABSTRACT

Background: cholangiocarcinoma requires accurate diagnosis, which relies on appropriate imaging and image-guided biopsy. Diffusion weighted MRI is a relative new and increasingly used technique. It can be obtained during a single breath-hold, there is no need to use contrast media and it provides information that reflects tissue cellularity and organization. ADC maps can provide quantitative measurements of tissue water diffusivity. It proved to be helpful in the characterization of cholangiocarcinoma.

Keywords: magnetic resonance imaging; diffusion weighted imaging; biliary tract, cholangiocarcinoma, characterization.

INTRODUCTION

Diffusion-weighted magnetic resonance imaging (DWI) provides information on the random (Brownian) motion of water molecules in the body. It is well established that DWI is a useful tool for the evaluation of intracranial diseases, such as acute stroke. The development of phased-array surface coils, high-gradient amplitudes and rapid imaging techniques such as echo planar imaging (EPI) and parallel imaging have been instrumental in allowing the extracranial application of DWI[(1-3).] The degree of restriction to water diffusion in biological tissues is directly proportional to tissue cellularity and the integrity of cell membranes. In tissues with a high cell density and associated with many intact cell membranes, such as malignant tumors, the motion of water molecules is more restricted than in less cellular tissue. The degree of water motion is found to be proportional to the degree of signal attenuation in DWI. Thus, more cellular solid tumors show relatively higher signal intensities and exhibit lower apparent diffusion coefficient (ADC, expressed in mm2/s) values on DWI using two or more b values than do less cellular tissues. Recently, this utility of DWI has been expanded to examination of abdominal organs; the ADC values of malignant masses are significantly lower than those of benign masses in the liver, pancreas, kidney, and prostate, although there is a small degree of overlap [4-9]. Most previous studies on DWI have been limited to the evaluation of diffuse parenchymal abnormalities and focal lesions in abdominal organs, whereas there are few studies about DWI for the evaluation of the biliopancreatic tract [10]. To date, contrast-enhanced magnetic resonance imaging (MRI) combined with magnetic resonance cholangiopancreatography (MRCP) has been found to be accurate for diagnosis of biliopancreatic diseases. The role of DWI for the evaluation of biliopancreatic diseases is not yet well established. However, because DWI yields qualitative and quantitative information reflecting cell membrane integrity and tissue cellularity, DWI can be used to differentiate normal and abnormal structures of tissues better, and thus may help in the characterization of various abnormalities in the biliopancreatic tract when added to conventional MRI [11]. In this article, we briefly reviewed the basic concepts for the biological basis of DWI and its technical considerations.

Additionally, we illustrated clinical applications of DWI for the following: evaluation of the biliopancreatic tract, including stone-related complications such as acute cholangitis, hepatic abscesses, and acute gallstone pancreatitis; characterization and diagnosis of gallbladder lesions, including cholecystitis, gallbladder empyema and gallbladder carcinoma; characterization of intrahepatic biliary lesions and diagnosis of malignant lesions in the intrahepatic bile ducts; and characterization of extrahepatic biliary lesions and diagnosis of malignant lesions in the extrahepatic bile ducts, including extrahepatic cholangiocarcinoma, pancreatic carcinoma, and focal pancreatitis.

BASIC CONCEPTS

In biological tissue, the diffusion of water molecules is impeded or restricted by natural barriers, such as cell membranes, large protein molecules, and tissue cellularity. Pathological conditions, such as tumors, cytotoxic edema,

Received: 12 / 6 /2017
Accepted:21 /6 /2017
DOI : 10.12816/0040118

abscesses, and fibrosis, in which the physical nature of the intracellular and extracellular spaces changes, result in increased restriction of the diffusion of water molecules. In tissues of low cellularity or where the cellular membranes have been disrupted, the diffusion of water molecules is relatively free or less restricted (**Figure 1**)[1-3,8,11].

DWI is typically obtained using an ultrafast T2-weighted single-shot spin-echo EPI sequence by applying a symmetric pair diffusion-sensitizing gradient, known as the Stejskal-Tanner sequence. It provides information on the random (Brownian) motion of water molecules in tissues between the first dephasing (diffusion-sensitizing) gradient and the second rephasing gradient on either side of the 180° refocusing pulse. Static molecules acquire phase information from the first diffusion-sensitizing gradient, but information will be cancelled out by the second gradient. As a result, signal intensity is preserved, with the exception of T2 decay.

In contrast, less restricted water molecules move a considerable distance between the first dephasing (diffusion-sensitizing) and second rephrasing gradients. The moving water molecules are not entirely rephased, resulting in reduction of the overall T2 signal intensity (Figure 2)[1-3].

The sensitivity of a DWI sequence to water diffusion can be altered by changing the parameter known as the b value, which represents the diffusion factor (measured in s/mm2) and the strength of the diffusion gradients. DWI is obtained with at least two different b values. DWI using lower b values (50-100 s/mm2) is sensitive only to fast motion of water molecules. On DWI using lower b values, water molecules in vessels are depicted as dark blood flow (black-blood images). DWI using higher b values (> 500 s/mm2) is sensitive to both fast and slow motion of water molecules. Water movements in highly cellular tissue are restricted and retain their signals even at higher b values. The images obtained at different b values allow the quantification of the ADC of tissues, which is usually displayed as a parametric (ADC) map.

The mean or median ADC value can be measured by drawing regions of diffusion and high cellular density show low ADC values, whereas tissues with less cellular density show higher ADC values[1,2].

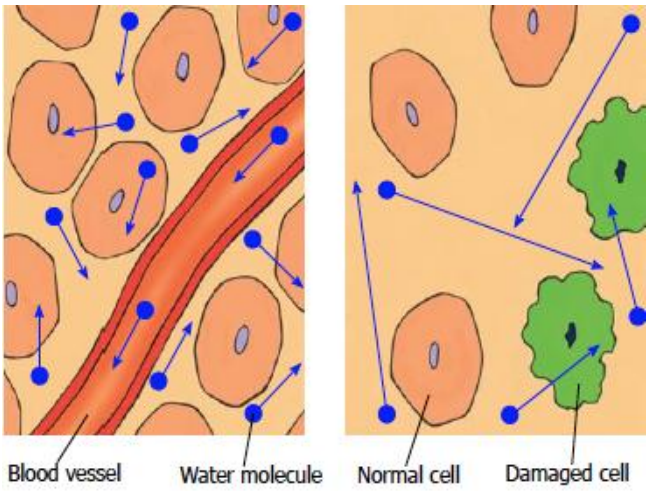

Figure 1: diffusion of water molecules. Highly cellular tissues with intact cell membrane restrict the movement of water molecules within intravascular, intracellular, and extracellular space. In contrast, relatively less cellular tissues or damaged cells with defective cellular membrane increase extracellular space, which allow greater water molecule movement.

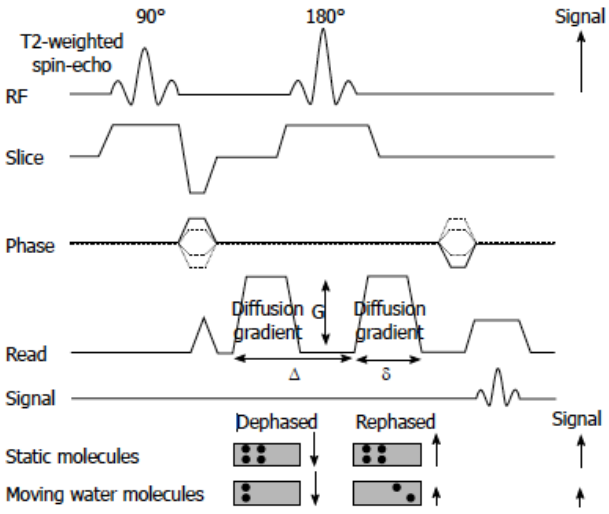

Figure 2: diagram of diffusion-weighted sequence. DWI is based on T2- weighted spin-echo sequencing with application of two equal gradient pulses (a dephasing gradient and a rephasing gradient) on each side of the 180° radiofrequency pulse. Static molecules are dephased by the first diffusion gradient and rephased perfectly by the second diffusion gradient; therefore, measured high signal intensity is preserved. In contrast, moving molecules undergo dephasing but are not entirely rephased by the second gradient because of their motion, thereby resulting in signal loss. DWI:

Diffusion-weighted magnetic resonance imaging; RF: Radiofrequency.

TECHNICAL CONSIDERATIONS

The signal intensity on DWI is dependent on diffusion of water molecules and T2 relaxation time. Thus, an area with a very long T2 relaxation time (e.g., bile in the biliary tract) maintains high signals on high-b-value DWI, and can be mistaken for restricted diffusion. This phenomenon is known as the "T2 shine-through" effect (Figure 3). The T2 shine-through effect inevitably confounds DWI images, and the ADC map eliminates this effect. In clinical practice, higher-b-value DWI (usually 800-1000 s/mm2) results in a reduction of the signal from moving protons in the bile ducts, cyst, vessels, and fluid in the bowel. This leads to a reduction in the T2 shine-through effect, resulting in increased contrast between lesions and visceral organs such as the liver or gallbladder. However, the tradeoffs of higher-b-value DWI are a lower signal-to-noise ratio, the possibility of ADC error, and increased image distortion due to the longer echo time required [1,2,8,12].

Figure 3: DWI of the normal liver, pancreas and biliary tract. A: DWI at b = 50 s/mm2 shows that the liver is hypointense compared to the kidney and spleen, and isointense compared to the pancreas; there is a signal void within the portal vein (arrow). DWI using low b values results in decreasing signals of fast motion of water molecules, such as that occurring within vessels. Such images are referred to as black-blood images; B: DWI at b = 500 s/mm2 shows that the signal intensity of bile is decreased (asterisk) and the wall of the gallbladder is not identified. The liver is isointense compared to the pancreas; C: DWI at b = 1000 s/mm2 shows a significant reduction in the signal intensity of bile in the gallbladder (asterisk). DWI: Diffusion-weighted magnetic resonance imaging.

DWI performed during free breathing can lead to substantial signal loss. Thus, breath-hold or respiration triggered DWI would be necessary to prevent signal loss as a result of respiratory movement. Breath-hold DWI is generally used because of its short acquisition time. However, only a limited number of image sections of relatively large section thicknesses can be acquired. Moreover, because this technique is usually performed using a single-shot EPI technique, the signal-to-noise ratio and lesion conspicuity is reduced. In contrast, respiration- triggered DWI provides higher signal-to-noise and contrast-to-noise ratios, although its acquisition time is longer than that of breath-hold DW I[13,14]. Fat suppression is necessary to increase the dynamic range of DWI and reduce the chemical shift artifacts that are prevalent in EPI. Inversion recovery sequence is preferred when performing DWI over a large area of the body, because it is likely to produce more uniform fat suppression [13]. Unlike brain imaging where b values are well established, b values in other parts of the body vary widely between investigators. Thus, b values for body imaging require optimization. Biexponential signal intensity in the abdominal organs has been shown in DWI with increasing b values; the initial rapid decrease in signal intensity is noted with a small increase in b value, and is followed by a more gradual decrease of signal intensity beyond approximately b = 100 s/mm2. ADC measurement using at least three b values adequately reflects this biexponential behavior, compared with the use of only two b values. Low b values are sensitive to capillary perfusion, which can increase the amount of perfusion contamination in ADC measurement. In

contrast, high b values enable less perfusion contamination in the ADC measurement and reflect tissue sensitivity[13]. For DWI, respiration-triggered, fat-suppressed, single-shot EPI is performed in the transverse plane with a parallel imaging (generalized auto-calibrating partially parallel acquisition) acceleration factor of two. DWI is performed prior to the intravenous injection of gadolinium chelates. Pre-contrast DWI is usually preferred because gadolinium chelates may affect the ADC values by decreasing the signal intensity on these T2-sequences due to shortening of the T1 and T2 relaxation time. However, it has been reported that DWI after administration of gadolinium chelates does not appear to affect ADC values significantly [15]. The imaging parameters of DWI in the 1.5-T unit are as follows: 5000/103 (repetition time ms/echo time ms), 90° flip angle, 4-mm section thickness, 1-mm intersection gap, 964-Hz/pixel bandwidth, 20 slices, 230-mm field of view, 192 × 192 matrix, and 85-s acquisition time. Imaging parameters in the 3.0-T unit are as follows: 3900/92 (repetition time ms/echo time ms), 90° flip angle, 5-mm section thickness, 0.5-mm intersection gap, 1184-Hz/pixel bandwidth, 24 slices, 230-mm field of view, 192 × 192 matrix and 85-s acquisition time. Each acquisition is obtained using five different b values including low values (0 s/mm2 and 50 s/mm2) and high values (500 s/mm2, 800 s/mm2 and 1000 s/mm2)[16,17].The ADC map is generated automatically. The signal intensity of the normal liver on DWI is the same as on T2-weighted images. The liver is hypointense compared to the kidney and spleen, and isointense or hypointense compared to the pancreas (Figure 3). The reported ADC value of the normal liver ranges from 1.02 × 10-3 mm2/s to 1.83 × 10-3 mm2/s [4,18-20]. **Yoshikawa *et al.*** [18] have reported that the mean ADC value of the pancreas ranges from 1.02 × 10-3 mm2/s to 1.94 × 10-3 mm2/s using DWI with two values (0 s/mm2 and 600 s/mm2). On higher DWI (usually 800-1000 s/mm2); walls of the bile duct and gallbladder are not identified (**Figure 3).**

DWI for characterization of intrahepatic biliary lesions and diagnosis of malignant lesions in the intrahepatic bile duct

Depending on their sites of origin, cholangiocarcinoma is classified as intrahepatic or extrahepatic. Based on its growth pattern, it is also classified as mass-forming, periductal-infiltrating, or intraductal-growing type. Intrahepatic cholangiocarcinoma originates from second order or greater peripheral branches of the intrahepatic bile duct. The mass-forming cholangiocarcinoma is the most common type of intrahepatic cholangiocarcinoma, but periductal-infiltrating and intraductal-growing intrahepatic cholangiocarcinoma was also seen [21,22]. Mass-forming intrahepatic cholangiocarcinoma appears as a single, predominantly homogeneous mass with well-circumscribed lobulated margins. Satellite nodules are frequent and vary in size. They usually appear as noncapsulated tumors, hypointense on T1-weighted images, and mild-to-moderately hyperintense on T2- weighted images, depending on the amount of fibrous tissue, necrosis, and mucin content. Dynamic-enhanced MRI reveals minimal-to-moderate initial peripheral rim enhancement followed by progressive and concentric incomplete filling of the tumor with contrast material [21]. In several studies, DWI is useful for detection of focal hepatic lesions, differentiation of cystic and solid hepatic lesions, and differentiation of benign and malignant focal hepatic lesions [4,19,23]. In one investigation using two b values (0 and 500 s/mm2), there were significant differences between the ADCs of benign and malignant focal hepatic lesions (2.45 ± 0.96 × 10-3 and 1.08 ± 0.50 × 10-3 mm2/s for b = 0 and 500 s/mm2, respectively; $P < 0.001$), although there was some overlap[4]. Mass-forming intrahepatic cholangiocarcinoma is usually large, achieving a diameter of up to 15 cm because early symptoms are rarely present. Thus, it is readily depicted on DWI and remains hyperintense on DWI using high b values with low ADC values; similar to values of other malignant focal hepatic lesions (**Figure 4)** [24]**.** Central hypointensity of the mass lesion may be seen on T2-weighted images and DWI using high b values, which may reflect fibrotic tissue in the central portion of the tumor. Peripheral hyperintensity can be demonstrated on DWI using high b values, corresponding to the more highly cellular region. As mentioned earlier, it is, however, difficult to distinguish mass-forming intrahepatic cholangiocarcinoma, hepatocellular carcinoma (HCC) and metastasis. Thus, DWI should be used along with conventional MRI sequences, such as dynamic-enhanced MRI, to differentiate mass-forming intrahepatic cholangiocarcinoma from other hepatic malignancies. Cholangiocarcinoma

tends to occur in atrophied or heavily stone-burdened segments. On cross-sectional images, it is difficult to diagnose cholangiocarcinoma associated with hepatolithiasis. A diagnosis of cholangiocarcinoma associated with hepatolithiasis should be considered when a mass involving or surrounding the bile duct is seen, or when focal nodular biliary wall thickening with increased enhancement is present in the region of the stricture [24]. DWI using high b values can be useful for the detection of cholangiocarcinoma associated with hepatolithiasis (**Figure 4).**

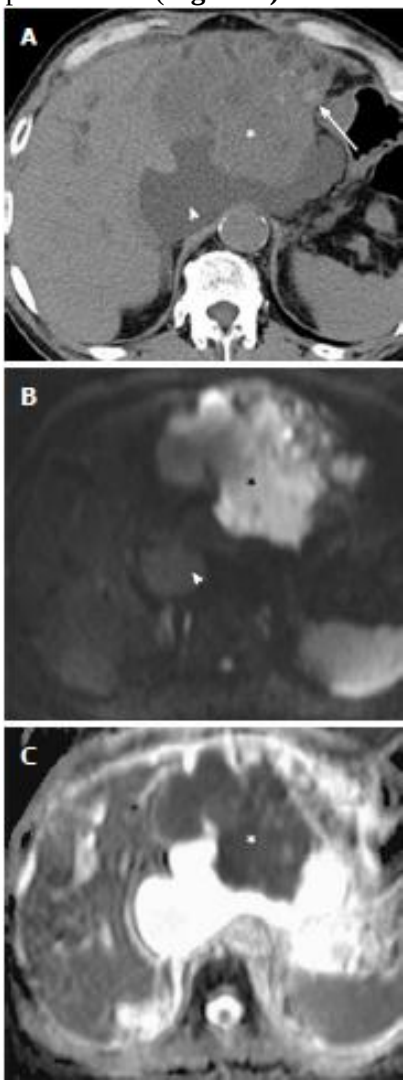

Figure 4: intrahepatic cholangiocarcinoma (mass-forming type) in a 71-year-old man. A: Non-enhanced CT image shows intrahepatic cholangiocarcinoma in the left lobe of the liver (asterisk), stones in the dilated left bile ducts (arrow), and a fluid collection in the lesser sac (arrowhead); B: DWI at b = 1000 s/mm2 shows intrahepatic cholangiocarcinoma with high signal intensity (asterisk). Note a fluid collection (arrowhead) in the lesser sac, which appears as significant attenuation of the signal intensity reduction at a high b value; C: On the ADC map, cholangiocarcinoma appears as low signal intensity (asterisk) due to restriction of diffusion. DWI: Diffusion-weighted magnetic resonance imaging; CT: Computed tomography; ADC: Apparent diffusion coefficient.

Diffuse periductal thickening along the bile duct in the periductal-infiltrating type, causing mild-to-marked bile duct dilatation, is seen in intrahepatic cholangiocarcinoma[21]. DWI may be helpful for the detection of malignant bile duct lesions causing a variable degree of intrahepatic bile duct dilatation, as well as for differentiating between intrahepatic malignant and benign bile duct lesions (**Figure 5).** Intraductal-growing cholangiocarcinoma appears as hyperintense intraluminal filling defects on DWI using high b values with low ADC values (**Figure 6).**

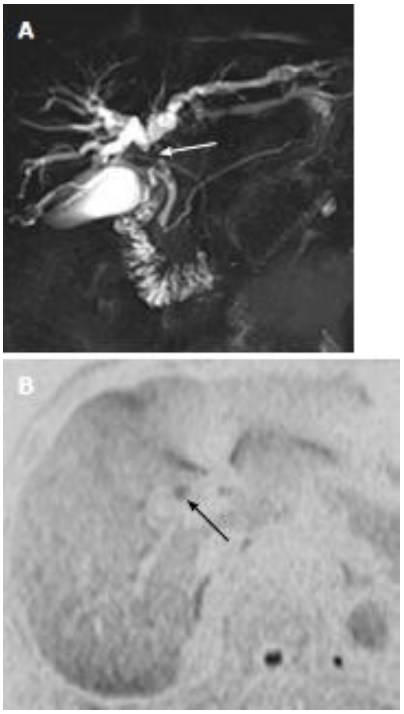

Figure 5: cholangiocarcinoma (periductal-infiltrating type) in a 70-yearold man. A: Coronal image from thick-slab, single-shot MRCP shows marked dilatation of the intrahepatic ducts and abrupt narrowing at the confluence of the hepatic duct (arrow); B: DWI at b = 800 s/mm2 with inverted black-and-white image contrast clearly depicts the mass (arrow) at the confluence of the

hepatic duct. DWI: Diffusion-weighted magnetic resonance imaging; MRCP: Magnetic resonance cholangiopancreatography.

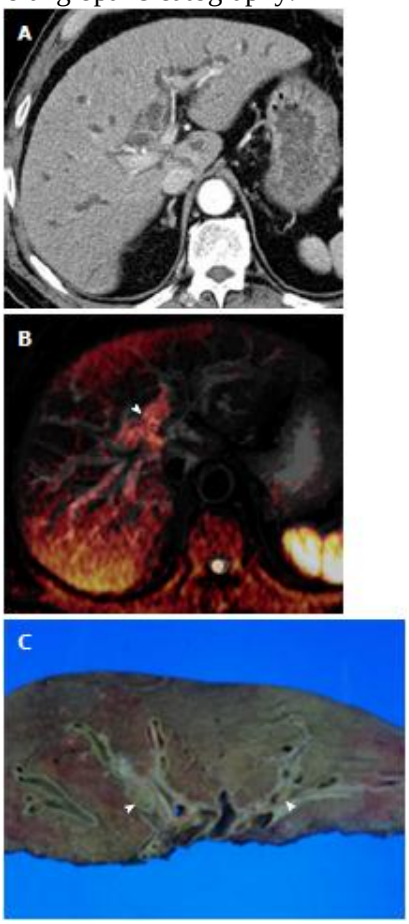

Figure 6: hilar cholangiocarcinoma (intraductal-growing type) in a 67-year-old man. A: Contrast-enhanced CT shows mild intrahepatic duct dilatation. However, intraductal masses are not clearly depicted on CT; B: Fusion image of T2-weighted and diffusion-weighted images at b = 800 s/mm2 shows high signal intensity (arrowhead) at the first branch of the intrahepatic duct; C: Photograph of the gross specimen shows intraductal growing masses (arrowheads) in the bile duct. Histological analysis revealed biliary intraepithelial neoplasia with high grade dysplasia. CT: Computed tomography.

However, detection of small malignant bile duct lesions is limited on DWI because tumor detection with DWI is affected by variable causes, such as low spatial resolution of higher-b-value DWI, tumor cellularity, bowel peristalsis, and artifacts. Invasion of the intrahepatic bile duct is infrequent in HCC, and seen in approximately 3.3%-9.0% of cases [25]. Obstruction of the bile duct in patients with HCC is caused by invasion of the intrahepatic bile duct, blood clots from the tumor, and tumor fragments. HCC with bile duct tumor thrombi can be distinguished from hematomas in the bile duct based on the presence of mass enhancement on dynamic-enhanced CT or MR I[26]. DWI can be useful for the differentiation of HCC and bile duct tumor thrombi from blood clots within the bile on the basis of identification of restricted diffusion of the mass lesion in the bile duct. They appear as hyperintense intraluminal filling defects on DWI using high b values with low ADC values (**Figure 7).**

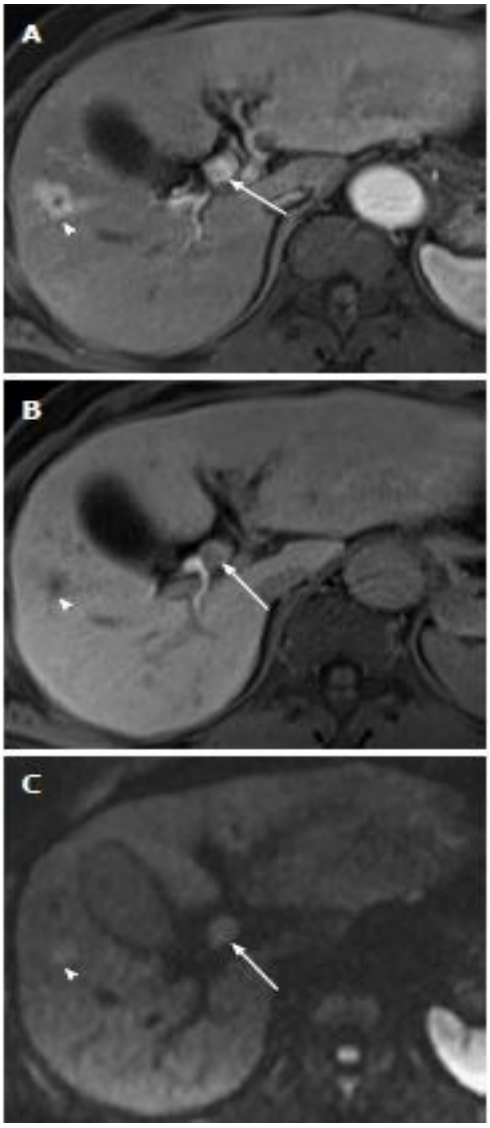

Figure 7: hepatocellular carcinoma with tumor thrombus in bile duct in a 62-year-old man. A: Gadoxetic acid-enhanced T1-weighted image obtained during the arterial phase shows a

hypervascular HCC in the right lobe of the liver (arrowhead) and an intraluminal enhancing mass (arrow) in the common hepatic duct; B: On gadoxetic-acid-enhanced T1-weighted image obtained 20 min after injection, a small HCC (arrowhead) is hypointense relative to the surrounding liver. Contrast material filling the left intrahepatic duct is delayed owing to a partial bile duct obstruction caused by tumor thrombus in the bile duct (arrow); C: DWI at b = 800 s/mm2 shows a hyperintense small HCC (arrowhead) and tumor thrombus in the bile duct (arrow). HCC: hepatocellular carcinoma.

However, because imaging findings of HCC with bile duct thrombi are similar to those of intraductal-growing cholangiocarcinoma, conventional MRI findings of a mass outside the ductal system, hypervascularity on dynamic imaging and underlying cirrhosis favor the diagnosis of HCC with bile duct tumor thrombi rather than Intraductal cholangiocarcinoma[27]. DWI for characterization of extrahepatic biliary lesions and diagnosis of malignant lesions in the extrahepatic bile duct Approximately two-thirds of extrahepatic bile duct cancer arises at the hepatic hilum (known as hilar cholangiocarcinoma or Klatskin tumor), and approximately one third originates from the distal common bile duct. The most common pattern of tumor growth is focal infiltration of the ductal wall or the periductal-infiltrating type, resulting in focal strictures. Other tumor growth patterns include the mass-forming and intraductal-growing types [21]. Extrahepatic bile duct carcinoma causes varying degrees of upstream bile duct dilatation. MRCP is highly accurate in identifying the presence and level of bile duct obstruction. Although differentiation between benign and malignant biliary lesions by MRCP is sometimes difficult, inspection of the bile duct lumen and wall on thin section images helps to identify malignancies, which often cause an eccentric, abrupt change in the bile duct caliber, with irregular shouldering at the transition point from large obstructed to small-caliber decompressed ducts. Benign strictures tend to show short-segment involvement with smooth, gradual, and concentric narrowing[28]. It has been reported that DWI is useful for the detection of extrahepatic cholangiocarcinoma and differentiation between malignant and benign biliary lesions. In a study using two b values (0 s/mm2 and 500 s/mm2), the sensitivity, specificity and accuracy of the detection of extrahepatic carcinoma were 94.3%, 100% and 96.4%, respectively [10]. On DWI using high b values, a high signal intensity with a low ADC value at the transition point from large obstructed to small-caliber decompressed ducts is a highly suggestive finding for malignant, rather than benign, biliary lesions because benign lesions usually show no hyper- or isointensity to the surrounding structures in the transitional area **(Figure 8).**

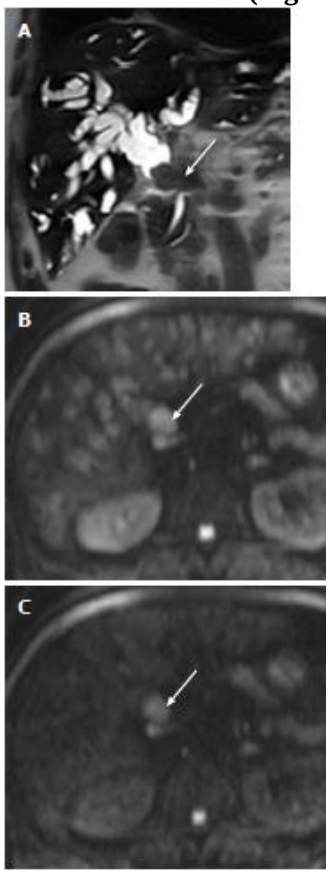

Figure 8: extrahepatic cholangiocarcinoma in a 62-year-old man. A: Coronal T2-weighted rapid acquisition relaxation enhancement image shows a mass (arrow) in the distal common bile duct and marked upstream bile duct dilatation; B: DWI at b = 800 s/mm2 shows a mass with high signal intensity (arrow), but the signal intensity of bile is also increased; C: DWI at b = 1000 s/mm2 shows a mass with high signal intensity (arrow). Note that the signal intensity of bile in the bile duct is significantly reduced. DWI: Diffusion-weighted magnetic resonance imaging. Thus, this finding can be a clue for differentiating between malignant and benign biliary lesions. However, there is some degree of overlap; benign active inflammatory conditions rarely have hyperintensity, and some

malignant lesions are not demonstrated on DWI using high b values [10]. Pancreatic carcinoma, cholangiocarcinoma, or chronic pancreatitis should be considered when a bile duct stricture is limited to the distal (intrapancreatic) common bile duct. Pancreatitis remains difficult to distinguish from pancreatic carcinoma on the basis of MRI findings, particularly in cases of acute or chronic mass-forming pancreatitis, because both appear as hypointense masses or mass-like lesions in the pancreas on T1-weighted images and are associated with ductal obstruction [29]. In a study using b values (0 s/mm2 and 600 s/mm2), DWI is helpful in detecting focal pancreatic lesions and differentiating between pancreatic carcinoma and mass-forming pancreatitis. Mass-forming pancreatitis has either lower or higher ADC values than pancreatic carcinoma, but ultimately follows the ADC values of the remaining pancreatic parenchyma, whereas the focal lesion in pancreatic carcinoma is invariably lower than the remaining parenchyma (**Figures 9 and 10**)[7].

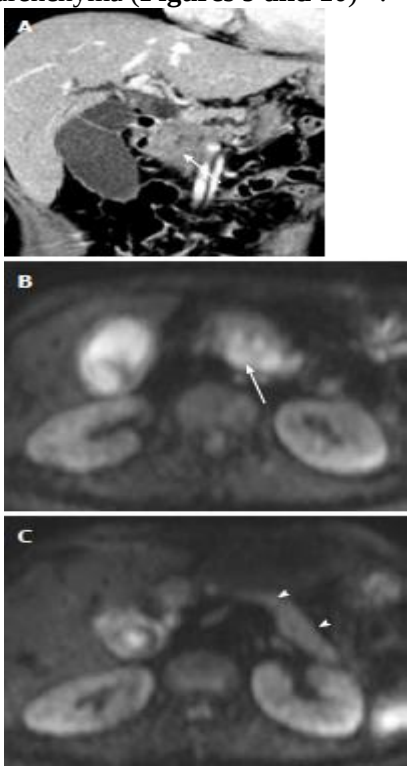

Figure 9: **pancreatic adenocarcinoma in a 50-year-old woman**. A: coronal reformatted contrast-enhanced CT image shows a double duct sign secondary to a pancreatic head cancer (arrow); B: On DWI at b = 800 s/mm2, pancreatic adenocarcinoma (arrow) shows hyperintensity; C: DWI at b = 800 s/mm2 superior to (B) shows high signal intensity of the remaining pancreas (arrowheads) due to obstructive pancreatitis. However, the remaining pancreas is less hyperintense relative to pancreatic adenocarcinoma. The ADC value of pancreatic cancer (1.23 ± 0.32 mm2/s) is significantly lower than that of the remaining pancreas (1.85 ± 0.45 mm2/s). DWI: Diffusion-weighted magnetic resonance imaging; CT: Computed tomography; ADC: apparent diffusion coefficient.

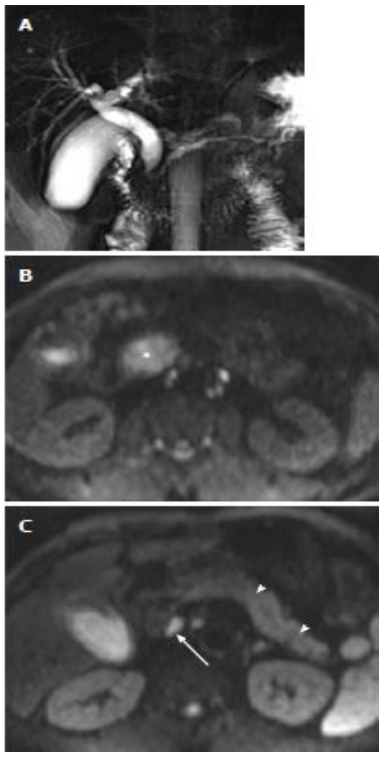

Figure 10: focal pancreatitis in a 52-year-old man. A: Coronal image from thick-slab single-shot MRCP shows a double duct sign with tapered narrowing of pancreatic duct in the head of the pancreas; B: On DWI at b = 800 s/mm2, focal pancreatitis (asterisk) shows hyperintensity; C: DWI at b = 800 s/mm2 superior to (B) shows high signal intensity of the remaining pancreas due to obstructive pancreatitis. The remaining pancreas is slightly hypointense (arrowheads) relative to pancreatic adenocarcinoma. The ADC value of focal pancreatitis (1.48 ± 0.16 mm2/s) is similar to that of the remaining pancreas (1.54 ± 0.28 mm2/s). Note a hyperintense reactive lymph node (arrow). DWI: Diffusion-weighted magnetic resonance imaging; MRCP: Magnetic resonance cholangiopancreatography; ADC: Apparent diffusion coefficient.

In a study using a high b value (1000 s/mm2), the sensitivity and specificity for the detection of pancreatic adenocarcinoma was 96.2% and 98.6%, respectively [30]. ADC values in pancreatic carcinoma tend to be lower than in the normal pancreas in most studies, although there is some degree of overlap [7,30]. Pancreatic carcinoma invokes a fibrotic response similar to desmoplastic reaction, therefore, ADC values are correlated with the degree of fibrosis; the ADC value of pancreatic carcinoma with loose fibrosis is higher than that of pancreatic carcinoma with dense fibrosis [31]. In a recent study, ADC at lower b values (< 500 s/mm2) was higher in mass-forming pancreatitis than in pancreatic carcinoma, whereas ADC at high b values was not significantly different between mass-forming pancreatitis and pancreatic carcinoma [17]. This was attributed to increasing perfusion effects at lower b values, which was correlated with high vascularity in chronic pancreatitis. Thus, DWI alone is suboptimal for the differentiation of pancreatic masses and mass-like lesions, and should be interpreted in conjunction with conventional MRI. Periampullary lesions have one or more of the following MRI features: the presence of biliary dilatation at the level of the ampulla of Vater with or without a dilated pancreatic duct, bulging of the papilla, a mass lesion in or around the ampulla of Vater, and abnormal enhancement of the papilla. It is not always easy to distinguish between neoplastic and non-neoplastic conditions in or around the ampulla of Vater using conventional MRI, because of the confusing or overlapping findings [32]. Ampullary or periampullary carcinoma displays mild-to-moderately high signal intensity on DWI using high b values with low ADC values, reflecting the high cellularity of tumors, whereas benign lesions, such as sphincter of Oddi dysfunction or papillary stenosis, show no high signal intensity in or around the ampulla of Vater (**Figures 11 and 12).** Thus, DWI can be helpful for detecting highly cellular malignant lesions and distinguishing between malignant and benign conditions in or around the ampulla of Vater. However, as mentioned earlier, some small malignant lesions in or around the ampulla of Vater are not identified on DWI using high b values.

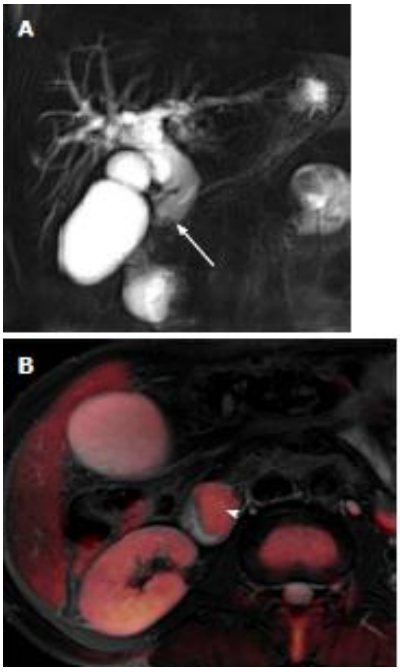

Figure 11: ampullary carcinoma in a 63-year-old man. A: Coronal image from thick-slab single-shot MRCP shows marked bile duct dilatation with abrupt narrowing (arrow) at the distal common bile duct; B: Fusion image of T2- weighted and diffusion-weighted imaging at b = 800 s/mm2 shows an ampullary mass with hyperintensity (arrowhead). MRCP: Magnetic resonance cholangiopancreatography.

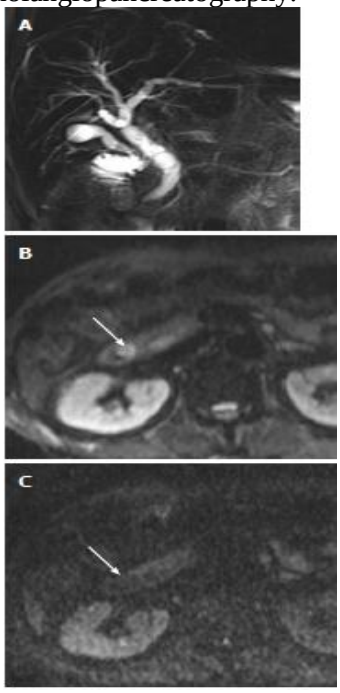

Figure 12: papillitis due to a recently passed stone in a 75-year-old man. A: Coronal image

from thick-slab single-shot MRCP shows mild bile duct dilatation; B: DWI at b = 50 s/mm2 shows a papilla with high signal intensity (arrow); C: On DWI at b = 800 s/mm2, the signal intensity of the papilla returns to the isosignal intensity (arrow). DWI: Diffusion-weighted magnetic resonance imaging; MRCP: Magnetic resonance cholangiopancreatography.

PITFALLS

DWI is susceptible to a variety of artifacts that arise from motion, use of strong gradient pulses, and EPI technique. Physiological motion artifacts such as respiratory motion, cardiac pulsation, movement of the diaphragm, and motility of the bowel lead to ghosting images and blurring. The pulsatile motion of the heart and aorta obscure or diminish visualization of and increase ADC in the left lobe of the liver. These artifacts can be overcome using respiratory or electrocardiographic triggering. The EPI technique produces a low spatial resolution and signal-to-noise ratio. The rapid on-and off switching of the high-intensity gradient field easily produce eddy currents, leading to geometrical distortion and image shearing artifacts that may become more pronounced with increased b values. DWI is also highly sensitive to magnetic field inhomogeneity.

Susceptibility artifacts caused by field inhomogeneity are prevalent at air-tissue interfaces or around tissue-metal interfaces[13,33]. Although restricted diffusion is generally considered to be associated with malignant lesions, some malignant lesions may not be detected on DWI. Some malignant tumors are too small for the DWI signal change to be obvious, or restriction to water diffusion is likely to be limited in malignant tumors with low cellularity, such as tumors with large cystic components. In contrast, some benign lesions sometimes exhibit restricted diffusion on imaging with high b values. The highly cellular tissue in reactive lymph nodes may show restricted diffusion (Figure 10). Thus, the role of DWI and ADC in distinguishing between benign and malignant lymph nodes remains unclear [34]. Additionally, diffusion of water in hematoma may be significantly restricted. Decreased ADC values in hemorrhage with intact red blood cell RBC) membranes (i.e., hyperacute, acute, and early subacute hematoma) and increased ADCs after lysis of RBC membranes (i.e., ‘‘free’’ methemoglobin in subacute-to-chronic hematoma) have been reported (Figure 13). This may be mistaken for malignant lesions on DWI or the ADC map, causing erroneous detection or characterization of lesions [35]. Thus, the radiologists have to be aware of potential pitfalls and limitation of the technique, and it should be kept in mind that DWI should be interpreted in conjunction with other conventional MRI.

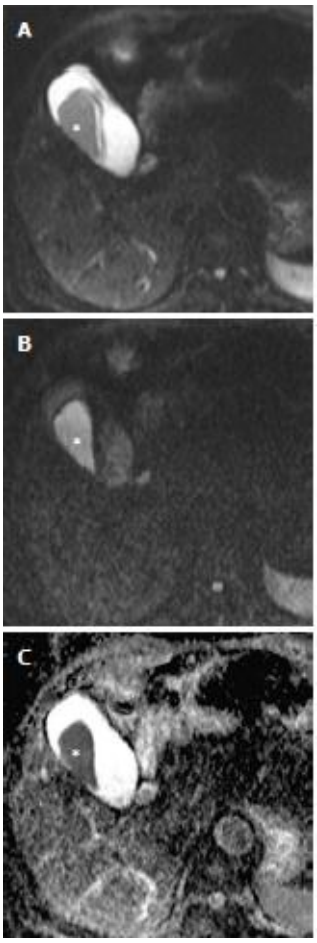

Figure 13: hemobilia secondary to percutaneous liver biopsy in a 55-yearold man.

A: DWI at b = 50 s/mm2 shows a hypointense hematoma in the gallbladder (asterisk); B: On DWI at b = 800 s/mm2, signal intensity of the hematoma changes to high signal (asterisk). C: On the ADC map, the hematoma in the gallbladder appears as low signal intensity (asterisk), which is associated with intact RBC membranes (i.e., hyperacute, acute, and early subacute hematomas). DWI: Diffusion-weighted magnetic resonance imaging; ADC: Apparent diffusion coefficient; RBC: Red blood cell.

CONCLUSION

Cholangiocarcinomas with variable growth pattern and location, along with overall poor prognosis, present eminent diagnostic challenges, in both detection and pre-operative staging of the disease as well as management.

Today, state-of-the-art MR imaging comprising a comprehensive imaging protocol of the liver, biliary tract and pancreas as well as the regional abdomen with dynamic contrast-enhanced MRI/MRA, MRCP, and DWI, is the modality of choice for diagnosis and resectability assessment as well as surveillance for cholangiocarcinoma in high risk population.

DWI can complement morphological information obtained by conventional MRCP by providing additional functional information concerning the alteration of tissue cellularity due to pathological processes. The detection of cholangiocarcinoma and the differentiation of malignant from benign tumor-like lesions in the biliopancreatic tract can be improved by combined evaluation using both DWI and conventional MRI. Moreover, DWI can be a reasonable alternative technique for the assessment of the biliopancreatic tract in the setting of a contraindication to contrast agents such as renal insufficiency or contrast allergy.

REFERENCES

1. **Koh DM and Collins DJ (2007):** Diffusion-weighted MRI in the body: applications and challenges in oncology. Am. J. Roentgenol., 188: 1622-1635.
2. **Qayyum A (2009)**: Diffusion-weighted imaging in the abdomen and pelvis: concepts and applications. Radiographics, 29: 1797-1810.
3. **Thoeny HC, De Keyzer F (2007):** Extracranial applications of diffusion-weighted magnetic resonance imaging. Eur Radiol., 17: 1385-1393
4. **Taouli B, Vilgrain V, Dumont E, Daire JL, Fan B and Menu Y (2003):** Evaluation of liver diffusion isotropy and characterization of focal hepatic lesions with two single-shot echo-planar MR imaging sequences: prospective study in 66 patients. Radiology, 226: 71-78.
5. **Parikh T, Drew SJ, Lee VS, Wong S, Hecht EM, Babb JS, Taouli B (2008):** Focal liver lesion detection and characterization with diffusion-weighted MR imaging: comparison with standard breath-hold T2-weighted imaging. Radiology, 246: 812-822
6. **Matsuki M, Inada Y, Nakai G, Tatsugami F, Tanikake M, Narabayashi I, Masuda D, Arisaka Y, Takaori K, Tanigawa N (2007):** Diffusion-weighed MR imaging of pancreatic carcinoma. Abdom Imaging, 32: 481-483 7
7. **Fattahi R, Balci NC, Perman WH, Hsueh EC, Alkaade S, Havlioglu N, Burton FR (2009):** Pancreatic diffusion-weighted imaging (DWI): comparison between mass-forming focal pancreatitis (FP), pancreatic cancer (PC), and normal pancreas. J Magn Reson Imaging, 29: 350-356 8
8. **Saremi F, Knoll AN, Bendavid OJ, Schultze-Haakh H, Narula N, Sarlati F (2009):** Characterization of genitourinary lesions with diffusion-weighted imaging. Radiographics, 29: 1295-1317
9. **Zhang J, Tehrani YM, Wang L, Ishill NM, Schwartz LH, Hricak H (2008):** Renal masses: characterization with diffusion weighted MR imaging--a preliminary experience. Radiology, 247: 458-464
10. **Cui XY, Chen HW (2010):** Role of diffusion-weighted magnetic resonance imaging in the diagnosis of extrahepatic cholangiocarcinoma. World J Gastroenterol., 16: 3196-3201
11. **Patterson DM, Padhani AR, Collins DJ (2008):** Technology insight: water diffusion MRI--a potential new biomarker of response to cancer therapy. Nat Clin Pract Oncol., 5: 220-233
12. **Whittaker CS, Coady A, Culver L, Rustin G, Padwick M, Padhani AR (2009**): Diffusion-weighted MR imaging of female pelvic tumors: a pictorial review. Radiographics., 29: 759-774.
13. **Koh DM, Takahara T, Imai Y, Collins DJ (2007):** Practical aspects of assessing tumors using clinical diffusion-weighted imaging in the body. Magn Reson Med Sci., 6: 211-224
14. **Kandpal H, Sharma R, Madhusudhan KS, Kapoor KS (2009**): Respiratory-triggered versus breath-hold diffusion-weighted MRI of liver lesions: comparison of image quality and apparent diffusion coefficient values. AJR Am J Roentgenol., 192: 915-922.
15. **Chiu FY, Jao JC, Chen CY, Liu GC, Jaw TS, Chiou YY, Hsu FO, Hsu JS (2005):** Effect of intravenous gadolinium-DTPA on diffusion-weighted magnetic resonance images for evaluation of focal hepatic lesions. J Comput Assist Tomogr., 29: 176-180
16. **Thoeny HC, De Keyzer F, Oyen RH, Peeters RR (2005):** Diffusion weighted MR imaging of kidneys in healthy volunteers and patients with parenchymal diseases: initial experience. Radiology, 235: 911-917
17. **Klauss M, Lemke A, Grünberg K, Simon D, Re TJ, Wente MN, Laun FB, Kauczor HU, Delorme S, Grenacher L, Stieltjes B (2011):** Intravoxel incoherent motion MRI for the differentiation between mass forming chronic pancreatitis and pancreatic carcinoma. Invest Radiol., 46: 57-63
18. **Yoshikawa T, Kawamitsu H, Mitchell DG, Ohno Y, Ku Y, Seo Y, Fujii M, Sugimura K (2006):** ADC measurement of abdominal organs and lesions using

parallel imaging technique. AJR Am J Roentgenol ., 187: 1521-1530

19. **Bruegel M, Holzapfel K, Gaa J, Woertler K, Waldt S, Kiefer B, Stemmer A, Ganter C, Rummeny EJ (2008):** Characterization of focal liver lesions by ADC measurements using a respiratory triggered diffusion-weighted single-shot echo-planar MR imaging technique. Eur Radiol., 18: 477-485
20. **Kim T, Murakami T, Takahashi S, Hori M, Tsuda K, Nakamura H (1999):** Diffusion-weighted single-shot echoplanar MR imaging for liver disease. AJR Am J Roentgenol., 173: 393-398
21. **Chung YE, Kim MJ, Park YN, Choi JY, Pyo JY, Kim YC, Cho HJ, Kim KA, Choi SY (2009):** Varying appearances of cholangiocarcinoma: radiologic-pathologic correlation. Radiographics, 29: 683-700
22. **Lim JH (2003):** Cholangiocarcinoma: morphologic classification according to growth pattern and imaging findings. AJR Am J Roentgenol., 181: 819-827
23. **Moteki T, Horikoshi H, Oya N, Aoki J, Endo K. (2002):** Evaluation of hepatic lesions and hepatic parenchyma using diffusion weighted reordered turbo FLASH magnetic resonance images. J Magn Reson Imaging., 15: 564-572
24. **Park HS, Lee JM, Kim SH, Jeong JY, Kim YJ, Lee KH, Choi SH, Han JK, Choi BI. (2006):** CT Differentiation of cholangiocarcinoma from periductal fibrosis in patients with hepatolithiasis. AJR Am J Roentgenol., 187: 445-453
25. **Wang HJ, Kim JH, Kim JH, Kim WH, Kim MW (1999):** Hepatocellular carcinoma with tumor thrombi in the bile duct. Hepatogastroenterology, 46: 2495-2499
26. **Jung AY, Lee JM, Choi SH, Kim SH, Lee JY, Kim SW, Han JK, Choi BI (2006):** CT features of an intraductal polypoid mass: Differentiation between hepatocellular carcinoma with bile duct tumor invasion and intraductal papillary cholangiocarcinoma. J Comput Assist Tomogr, 30: 173-181
27. **Gabata T, Terayama N, Kobayashi S, Sanada J, Kadoya M, Matsui O (2007):** MR imaging of hepatocellular carcinomas with biliary tumor thrombi. Abdom Imaging, 32: 470-474
28. **Park MS, Kim TK, Kim KW, Park SW, Lee JK, Kim JS, Lee JH, Kim KA, Kim AY, Kim PN, Lee MG, Ha HK (2004):** Differentiation of extrahepatic bile duct cholangiocarcinoma from benign stricture: findings at MRCP versus ERCP. Radiology, 233: 234-240
29. **Johnson PT, Outwater EK (1999):** Pancreatic carcinoma versus chronic pancreatitis: dynamic MR imaging. Radiology, 212: 213-218
30. **Ichikawa T, Erturk SM, Motosugi U, Sou H, Iino H, Araki T, Fujii H (2007):** High-b value diffusion-weighted MRI for detecting pancreatic adenocarcinoma: preliminary results. AJR Am J Roentgenol., 188: 409-414
31. **Muraoka N, Uematsu H, Kimura H, Imamura Y, Fujiwara Y, Murakami M, Yamaguchi A, Itoh H (2008):** Apparent diffusion coefficient in pancreatic cancer: characterization and histopathological correlations. J Magn Reson Imaging, 27: 1302-1308
32. **Kim TU, Kim S, Lee JW, Woo SK, Lee TH, Choo KS, Kim CW, Kim GH, Kang DH (2008):** Ampulla of Vater: comprehensive anatomy, MR imaging of pathologic conditions, and correlation with endoscopy. Eur J Radiol., 66: 48-64
33. **Le Bihan D, Poupon C, Amadon A, Lethimonnier F (2006):** Artifacts and pitfalls in diffusion MRI. J Magn Reson Imaging, 24: 478-488
34. **Feuerlein S, Pauls S, Juchems MS, Stuber T, Hoffmann MH, Brambs HJ, Ernst AS (2009):** Pitfalls in abdominal diffusion-weighted imaging: how predictive is restricted water diffusion for malignancy. AJR Am J Roentgenol., 193: 1070-1076
35. **Atlas SW, DuBois P, Singer MB, Lu D (2000):** Diffusion measurements in intracranial hematomas: implications for MR imaging of acute stroke. AJNR Am J Neuroradiol., 21: 1190-1194.